A STUDY OF MULTIPACTING EFFECTS IN LARGE CYCLOTRON CAVITIES BY MEANS OF FULLY 3-DIMENSIONAL SIMULATIONS*

Chuan Wang#, Bin Ji, Pengzhan Li, Zhiguo Yin, Yu Lei, Jiansheng Xing, Tianjue Zhang,
CIAE, Beijing, China
Andreas Adelmann, Achim Gsell, Mike Seidel, PSI, Villigen PSI, Switzerland

Abstract

Field emission model and secondary emission models, as well as 3D boundary geometry handling capabilities, are needed to efficiently and precisely simulate multipacting phenomena. These models have been implemented in OPAL, a parallel framework for charged particle optics in accelerator structures and beam lines. The models and their implementation are carefully benchmarked against a non-stationary multipacting theory. A dedicated multipacting experiment with nanosecond time resolution for the classic parallel plate geometry has also shown the validity of the OPAL model.

Multipacting phenomena, in the CYCIAE-100 cyclotron, under construction at the China Institute of Atomic Energy, are expected to be more severe during the RF conditioning process than in separate-sector cyclotrons. This is because the magnetic stray fields in the valley are stronger, which may make the impact electrons easier to reach energies that lead to larger multipacting probabilities. We report on simulation results for CYCIAE-100, which gives us an insight view of the multipacting process and help to develop cures to suppress these phenomena.

INTRODUCTION

Multipacting phenomena have been observed in various RF structures of accelerators. Multipacting is appearing in high-Q RF cavities of cyclotrons [1, 2]. The primary or seed electrons will impact the cavity surface, and produce an avalanche of secondary electrons. Under certain conditions (material and geometry of the RF structure, frequency etc.), the electron secondary emission yield (SEY) coefficient will be larger than one and lead to exponential multiplication of electrons. This kind of discharge will limit the power level until the surfaces will be cleaned through a very time-consuming conditioning process [1, 2]. The appearance of magnetic field in cyclotrons will make the impact electrons easier to reach energies that lead to larger secondary emission yields and make the prediction of electron trajectories in cyclotron cavities more difficult. Large scale multipacting simulations based on reliable data of surface material, full size geometry of RF structures and parallel computing allow more thorough analysis and a deeper understanding of these phenomena even in early design stage of RF structures. To make OPAL [3] a feasible tool to perform these large scale multipacting simulations, first we

implement a 3D particle-boundary collision test model into OPAL. We have implemented surface physics models including two secondary emission models, developed by Furman-Pivi and Vaughan respectively. The above mentioned models and their implementation in OPAL have been benchmarked against both a non-stationary theory [4] and a nanosecond time resolved multipacting experiment with a parallel plate geometry. The time evolution of the particle density among simulation, theory and experiment agrees very well.

MODEL IMPLEMENTATIONS IN OPAL

Geometry Handling

The particle-boundary collisions test is crucial to multipacting simulations. Since complex 3D geometries are hard to be accurately parameterized by simple functions, we use oriented triangulated surfaces, which are extracted from volume mesh generated by GMSH [5], to represent the complex geometry of real RF structures. Subsequently we can make use of efficient 3D line segment-triangle intersection (LSTI) tests [6] to find exact locations of particle-boundary collisions. Even though the implemented LSTI algorithm use pre-computed oriented triangles, early rejection strategy is necessary to bring the computational time down to an acceptable level. By using an early rejection strategy (see Fig. 1), the number of LSTI tests in each time step has been greatly reduced. In that example, only the red particles will be tested in each time step. If we have M triangles and N particles in the simulation, both in the magnitude of tens of thousands to millions, the number of LSTI tests in single time step without the described early rejection technique would be prohibitive. The details of this early rejection strategy have been documented in our previous reports [7].

Surface Physics Models

Electron field emission is a major source of primary particles in the secondary emission process. The Fowler-Nordheim (F-N) model has been used to model these seed electrons in OPAL [7].

We have implemented two secondary emission models. The first one is a phenomenological model developed by M.A. Furman and M. Pivi [8]. The Furman and Pivi's secondary emission model calculates the number of secondary electrons that results from an incident electron of a given energy on a material at a given angle. For each of the generated secondary electrons the associated process: true secondary, re-diffused or backscattered is recorded, as is sketched in Fig. 2
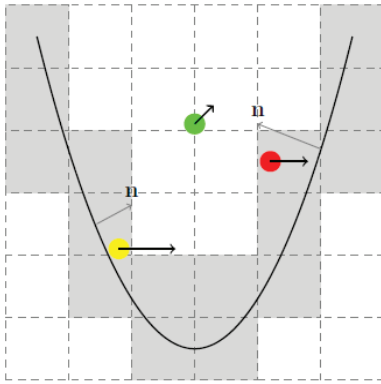
Figure 1: Schematic view of particle-boundary early rejection strategy. The dark black line represents the boundary surface; particles are colour dots with an attached momentum arrow and inward normal gray arrows.
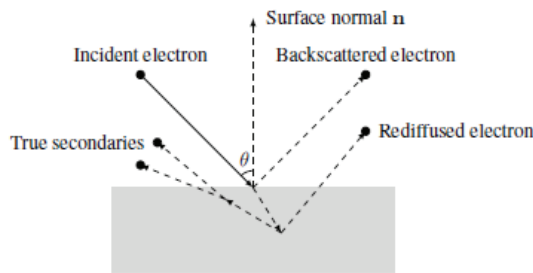
.

Figure 2: Sketch map of the secondary emission process

The other secondary emission model we use is based on a secondary emission yield model developed by Vaughan [9, 10].

Sometimes, the population of particles in simulation domain may continually grow exponentially, leading to an enormous amount of simulation particles, orders of magnitude larger than the initial number. To overcome this, a re-normalization procedure of simulation particles is developed. In each electron impact event, instead of emitting the real number of simulation particles predicted by secondary emission models, we emit only one particle, and renormalize the charge. This approach an accurate representation of the secondary emission models which can be seen in the following parallel plate benchmarking cases.

Code Benchmark against Theory and Experiment

The theory we used to benchmark above models is S. Anza's non-stationary multipacting theory [11]. This theory is restricted to a plane parallel plate with a homogeneous RF electric field in between, directed perpendicular to the plates and varying harmonically in time. This model can also predict the time resolution of

the electron multipacting, which can be directly compared with OPAL simulations.

The time evolution of electron number density under different frequencies, gap voltages and surface SEY curves have been calculated with both the none stationary theory and OPAL simulations. Both the two types of the secondary emission models and the re-normalization approach have been benchmarked. The results are shown in Fig. 3 and agree very well.
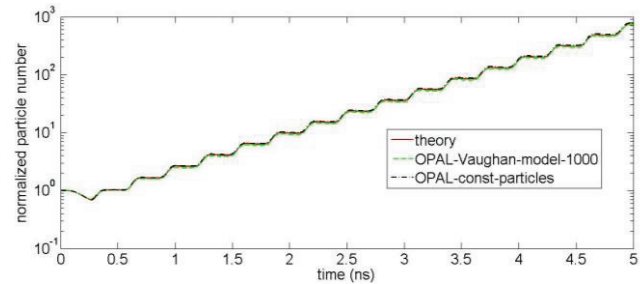

Figure 3: Time evolution of electron number at f =1640MHz, V_0 = 120V, d = 1mm, using Vaughan's model in simulation and silver's SEY data in theory.

To further benchmark the models in OPAL, we have performed a dedicated nanosecond time resolved multipacting experiment, on a λ/4 resonator at 73 MHz. The gap between two parallel circular copper plates is about 18 mm. The circuit model of the nanosecond time resolved measurement circuit is shown in Fig. 4. Using the simulated electron impacting rate at one plate as the current source, a SPICE based circuit simulation can predict the measured multipacting current pattern [12].
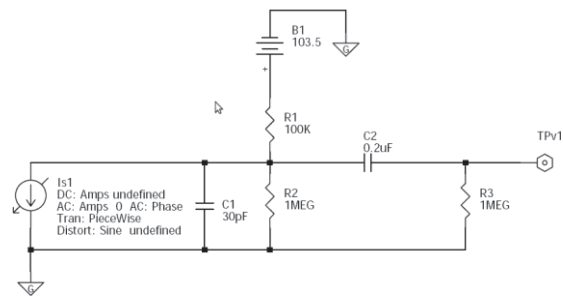

Figure 4: Circuit model of the time resolved measurement circuit.

RF CONDITIONING OF THE TEST CAVITY OF CYCIAE-100 CYCLOTRON

We have built and tested a 1:1 model of the copper cavity for CYCIAE-100. Several important experiments such as the measurement of the Q value and the RF conditioning test where done. The installation of the cavity and some multipacting observations are shown in Fig. 5 and Fig. 6.

Figure 5: The installation (left) and the traces of multipacting (the darker colour on the cavity surface) at the ends of the cavity.

Figure 6: The typical signal from pickups which gives the RF power in cavity (absorption due to multipacting).

These RF conditioning measurements are performed without magnetic field. Due to the appearance of magnetic fields in the valley of the magnet, the multipacting in the RF conditioning phase of the CYCIAE-100 cavities will become more severe.

MULTIPACTING SIMULATION OF THE CYCIAE-100 CAVITIES

Multipacting phenomena of the CYCIAE-100 H$^-$ AVF cyclotron under construction at the China Institute of Atomic Energy (CIAE) [13] are investigated. The accelerating voltage provided by the cavity of CYCIAE-100 is 60 kV ∼ 120 kV from inner radius to outer radius and the full power of one cavity is ∼ 30 kW.

The RF cavities will be installed in the valley of the cyclotron magnet and therefore will be exposed to magnetic stray fields of a few hundreds Gauss. It is worth to note, that this stray field is also modelled in the simulation, as shown in see Fig. 7.
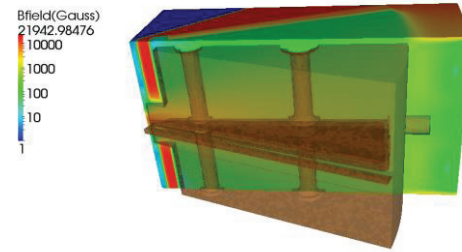

Figure 7: The RF cavity of CYCIAE-100 cyclotron with the magnetic stray field.

The electromagnetic field of the RF cavity of CYCIAE-100 has a maximum of 6.1 MV/m (see Fig. 8). In the simulation, different power level will be used. The initial electrons will be randomly generated near the surface of the cavity.
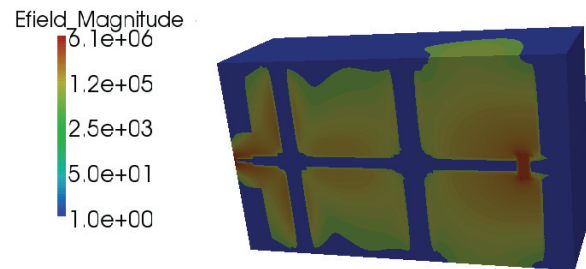

Figure 8: The electric field in the RF cavity of CYCIAE-100 cyclotron.

The Effect of SEY on the Multipacting Behaviour

According to experiments performed by CERN for LHC project, the SEY curve of copper can vary dramatically with different surface treatments [14]. It will be interesting to predict the multipacting phenomena in the conditions with or without surface treatment for the RF cavities of the CYCIAE-100. The SEY curves in Fig. 9 fit to the experimental data in Ref [14] with the Vaughan's secondary emission model and will be used in the simulations. The data in Fig. 9 are correspond to the SEY of copper without surface treatment and the SEY of copper with the most probable surface treatment and installation condition that we will use for the cavity, i.e., the sputter cleaned surface with several days exposure to air outside the vacuum chamber, respectively.
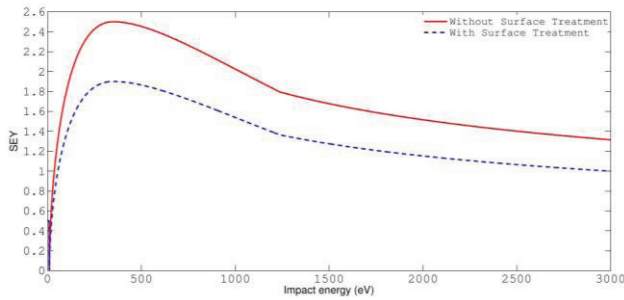
Figure 9: The SEY curve of copper used in the multipacting study (fitted by Vaughan's formula).

Multipacting has been observed with and without surface treatment. Data for one RF cycle, is show in Fig. 10.
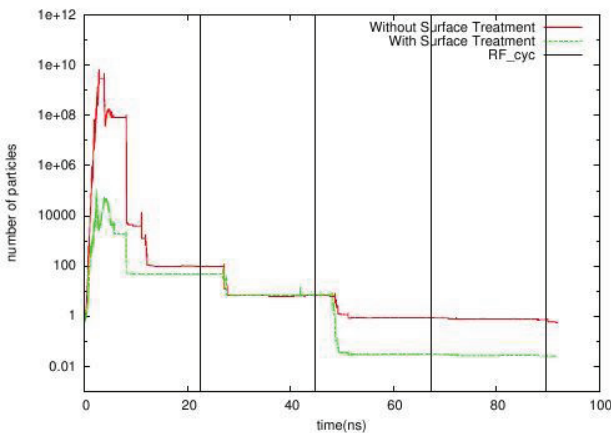

Figure 10: The time evolution of particle numbers in both with and without surface treatment cases.

The electron multiplication in the case without surface treatment is 5 orders of magnitude larger than the case with surface treatment, which clearly indicate the necessity of surface treatment.

RF Phase Lag Effects on the Multipacting Behaviour

To study whether the RF phase lag have an influence on the multipacting behaviour, we have to performed a parameter study, with seed electrons in the RF field at different phases. Typical results at full power level are shown in Fig. 11.

In most cases, the simulated electron number density is increasing within less than 1 RF cycle.

As show in Fig. 11, there exists cases for example at 75 deg of phase, in which the electron number density will continuously increase and hence the multipacting behaviour shows a phase dependences. This long time period multipacting must be taken care of.
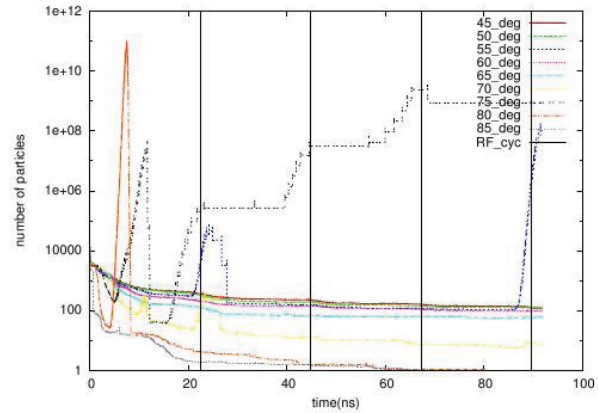

Figure 11: The time evolution of particle number density at different phases.

Visualization of the Multipacting Hot Zone

Motivated by the observations of traces of electron impinging on the surfaces, and also for better diagnosing the positions where multipacting happens, OPAL will dump the position and the current of incident particles into a file. Within H5hut framework [15], we can convert the H5 file to VTK files. These VTK files can be used to visualize the hot zones of the RF structure where multipacting happens. Hopefully this can be directly compared with the observations of electron impact traces on the surfaces of RF cavities. The simulated hot zone of the RF cavity at a lower power level is shown in Fig. 12.
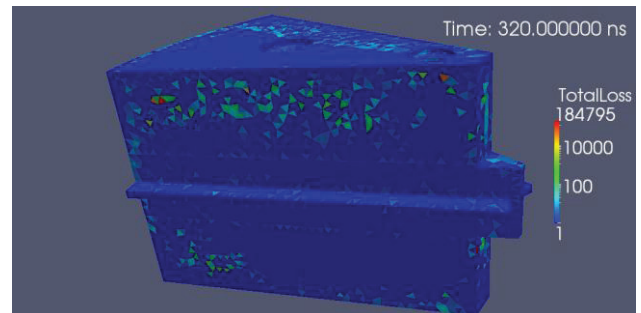

Figure 12: Simulated hot zone in the RF cavity of CYCIAE-100 cyclotron at 1/16 of the full RF power.

Possible Cure to Suppress the Multipacting

Multipacting in cyclotron cavities will cause the reflection of input RF power, and usually a lengthy RF conditioning process is needed to reach the required RF power in the cavity.

If we look into the mechanism of the RF conditioning process, the deposition of low SEY material on the cavity surface during electron impacting is believed to be a cure to the multipacting problem. Thus, coating the surfaces of RF cavity with low SEY material becomes a pretty straightforward idea. But the coating materials usually contain graphite powders, and using these coating materials in large area will probably damage the vacuum pumps. With the help of OPAL simulations, we hope to

get the correct positions where multipacting takes place, and thus we can greatly reduce the coating area and makes coating become applicable.

We are planning to use such a coating scheme at specific areas, according to simulation results during the RF conditioning of CYCIAE-100 cyclotron.

CONCLUSION

A non-stationary multipacting model is available and benchmarked w.r.t. theory and experiment, in the beam dynamics code OPAL.

The carefully performed benchmark against the non-stationary multipacting theory and a nanosecond time resolved experiment gives us strong confidence on the predictive nature of OPAL, as a tool for analysing multipacting phenomena in large RF structures.

The preliminary studies on the multipacting of the CYCIAE-100 cyclotron cavity on different RF power levels will help us to understand the multipacting behaviour during the RF conditioning process.

The identification of multipacting zones will enable us to use a localized coating procedure and hopefully shorten the time of RF conditioning.

REFERENCES

[1] P. K. Sigg, "Reliability of High Beam Power Cyclotron RF-Systems at PSI," Proceedings of the Workshop on Utilization and Reliability of High Power Proton Accelerators, Mito, Japan, 1998, http://rf.web.psi.ch/files/proceedings/1998/JAERI98/Paper NEA98.pdf

[2] N. Sakamoto et al., "RF-System for the RIBF Superconducting Ring Cyclotron," CYCLOTRONS'2007, Giardini Naxos, Italy, 2007.

[3] A. Adelman et al., "The OPAL (Object Oriented Parallel Accelerator Library) Framework," Paul Scherrer Institut, PSI-PR-08-02, 2008.

[4] S. Anza et al., Phys. Plasmas. 17 (2010) 6 062110.

[5] C. Geuzaine and J. F. Remacle, International Journal for Numerical Methods in Engineering. 79 (2009) 11 1309.

[6] D. Sunday, http://softsurfer.com/Archive/algorithm_0105/algorithm_0105.htm

[7] C. Wang et al., "A Field Emission and Secondary Emission Model in OPAL," HB2010, Morschach, Switzerland, 2010, MOPD55.

[8] M. A. Furman and M. T. F. Pivi, Phys. Rev. ST Accel.Beams, 5 (2002) 12 124404.

[9] J. R. M. Vaughan, IEEE Transactions on Electron Devices. 36 (1989) 9 1963.

[10] J. R. M. Vaughan, IEEE Transactions on Electron Devices. 40 (1993) 4 830.

[11] S. Anza et al., Phys. Plasmas. 17 (2010) 6 062110.

[12] C. Wang et al., arXiv:1208.6577 [physics.acc-ph]

[13] T. J. Zhang et al., NIM B. 266 (2008) 19 4117-4112.

[14] I. Bojko et al., "The Influence of Air Exposures and Thermal Treatments on the Secondary Electron Yield of Copper," LHC Project Report, CERN, 376 (2000).

[15] Mark Howison et al., "H5hut: A High-Performance I/O Library for Particle-based Simulations", IASDS10 – Workshop on Interfaces and Abstractions for Scientific Data Storage, Heraklion, Crete, Greece. September 2010.